Biochimica et Biophysica Acta 1827 (2013) 446–454

Contents lists available at SciVerse ScienceDirect

Biochimica et Biophysica Acta

journal homepage: www.elsevier.com/locate/bbabio

Partitioning of superoxide and hydrogen peroxide production by mitochondrial respiratory complex I

Vera G. Grivennikova, Andrei D. Vinogradov *

Department of Biochemistry, School of Biology, Moscow State University, Moscow 119991, Russian Federation

ARTICLE INFO

Article history:
Received 21 November 2012
Received in revised form 24 December 2012
Accepted 2 January 2013
Available online 10 January 2013

Keywords:
Respiratory complex I
Dihydrolipoamide dehydrogenase
Hydrogen peroxide
Superoxide anion
Pyridine nucleotides
Guanidine

ABSTRACT

Membrane-bound respiratory complex I in inside-out submitochondrial particles (SMP) catalyzes both superoxide and hydrogen peroxide formation in NADH- and/or succinate-supported reactions. At optimal NADH concentration (50 μM), the complex I-mediated process results in a formation of two superoxide anions and H_2O_2 as the reaction products in approximately 0.7 ratio. Almost the same ratio is found for purified complex I (0.6) and for the aerobic succinate-supported reverse electron transfer reaction. Superoxide production is depressed at high, more physiologically relevant NADH concentrations, whereas hydrogen peroxide formation is insensitive to the elevated level of NADH. The rates of H_2O_2 formation at variable NAD^+/NADH ratios satisfactorily fit the Nernst equation for a single reactive two-electron donor component equilibrated with ambient midpoint redox potential of −347 mV (0.13 NAD^+/NADH ratio, pH 8.0). Half-maximal superoxide production rate proceeds at significantly higher NAD^+/NADH ratio (0.33). Guanidine strongly stimulates NADH-supported hydrogen peroxide and superoxide production at any NADH concentration and activates NADH:ferricyanide and inhibits NADH:hexaammineruthenium (III) reductase activities while showing no effects on NADH oxidase of SMP. In the low range of NADH concentration, superoxide production rate shows a simple hyperbolic dependence on NADH with apparent K_m^{NADH} of 0.5 μM, whereas sigmoidal dependence of hydrogen peroxide production is seen with half-maximal rate at 25 μM NADH. We interpret the data as to suggest that at least two sites participate in complex I-mediated ROS generation: $FMNH^-$ that produces hydrogen peroxide, and an iron–sulfur center (likely N-2) that produces superoxide anion.

1. Introduction

The maximal relative contribution to the total cellular hydrogen peroxide production from various subcellular fractions of rat liver have been approximated as 15%, 45%, 35%, and 5% for mitochondria, microsomes, peroxisomes, and cytosolic enzymes, respectively [1]. Up to 2% of oxygen consumed by rat liver or pigeon heart mitochondria respiring in State 4 is converted to hydrogen peroxide, and this amount is drastically decreased at State 3 or upon uncoupling [2,3]. Thus under certain physiologically relevant conditions mitochondria are thought to contribute significantly to the steady-state level of hydrogen peroxide in cells [4–6].

About half of the total ROS (superoxide anion and hydrogen peroxide) produced by heart mitochondria at high NADH/NAD^+ ratio can be accounted for as being generated by the respiratory chain components (complex I and complex III) [7,8]. The rest is produced by soluble enzymes of the matrix, mostly by dihydrolipoamide dehydrogenase (DLDH) [8–11]. Inside-out bovine heart submitochondrial particles (SMP) essentially free of other than the respiratory chain ROS generators catalyze superoxide production during coupled respiration with either NADH or succinate at the rate corresponding to about 0.1% of oxygen consumed by cytochrome oxidase [12]. Inhibitory analysis suggests that the major part of superoxide produced by the respiratory chain (up to 70%) is generated by complex I [12].

Mammalian complex I is a gigantic iron–sulfur-flavo-lipoprotein composed of 44–45 different subunits [13,14] bearing at least ten redox components (FMN, eight iron–sulfur clusters, bound ubiquinone) [15]. As a component of the respiratory chain, the enzyme catalyzes reversible proton-translocating NADH:ubiquinone oxidoreduction, thus operating as an energy-transducing device (coupling site 1) [15]. All known redox components are buried in the hydrophilic domain of the enzyme exposed to the matrix space [16,17].

The mechanism of ROS production by complex I is of considerable interest because cellular oxidative stress is conventionally believed to be a major cause of a number of pathologies and the aging process [18–20]. Besides their biomedical importance, studies on ROS production by complex I may provide information on the arrangement and reactivity of its specific redox components. Which particular component(s) in the NADH-ubiquinone region of the respiratory chain directly interact(s) with oxygen is still debated: $NAD^{\bullet}$-radical [21], FMN [22–25], ubisemiquinone [26], and iron–sulfur clusters N-1a

Abbreviations: SMP, submitochondrial particles; $O_2^{\bullet-}$, superoxide anion; ROS, reactive oxygen species; FMN, flavin mononucleotide; DLDH, dihydrolipoamide dehydrogenase; HP, horseradish peroxidase; SOD, superoxide dismutase; HAR, hexaammineruthenium(III); Q_1, 2,3-dimethoxy,5-methyl,6-isoprenyl,1,4-benzoquinone; BSA, bovine serum albumin; FP, low mol. mass fragment of bovine heart complex I

* Corresponding author. Tel./fax: +7 495 939 13 76.
E-mail address: adv@biochem.bio.msu.su (A.D. Vinogradov).

0005-2728/$ – see front matter © 2013 Elsevier B.V. All rights reserved.
http://dx.doi.org/10.1016/j.bbabio.2013.01.002

[27] or N-2 [28] have been suggested as the species involved in ROS production. Also, a single site [25], two-sites [29], and dynamically shifted two sites/species [30] models have been proposed by different research groups.

An interesting feature of superoxide generation catalyzed by complex I bound to the coupling membrane in the presence of either NADH or succinate (via energy-linked reverse electron transfer) is that the reaction is strongly inhibited if the concentration of NADH increases above "optimal" with an apparent "K_i" in the μmolar range [12]. When hydrogen peroxide production was detected as ROS produced by complex I in the presence of superoxide dismutase (SOD), less inhibition by elevated NADH was observed. We thought that this apparent discrepancy could be explained if both superoxide and hydrogen peroxide are produced by complex I, and only the former process is inhibited by high concentrations of NADH. This paper describes experiments supporting this hypothesis. The effects of guanidine, a ligand known to strongly stimulate NADH:ferricyanide reductase activity of the enzyme [31,32] and to increase the flavin radical seen in complex I [33], on ROS production are also described. Possible mechanisms (sites) of complex I-oxygen interaction are discussed.

2. Materials and methods

Bovine heart SMP were prepared [34], coupled by treatment with oligomycin, and activated [35] according to published protocols. Bovine heart complex I was purified according to Hatefi et al. [36]. All the assays were done at 30 °C. Protein content was determined by the biuret procedure.

Trypsin-treated SMP were prepared as follows. Ten mg of trypsin was dissolved in 0.5 ml of the standard reaction mixture (see below), and 0.44 ml of this solution was added to 4 ml of SMP (22 mg/ml) suspended in the same medium (0.1 mg of trypsin per mg of SMP protein). The mixture was incubated on ice for 30 min. Trypsin inhibitor (44 mg of protein) was then added and incubated for 10 min. The mixture was diluted to 80 ml, and the SMP were sedimented (1 h at 30 000 g), washed with 80 ml of the standard mixture, suspended in 3 ml of the same medium, and stored as 0.25 ml samples in liquid nitrogen.

Hydrogen peroxide formation was measured photometrically with Amplex Red (20 μM) as a formation of resorufin, $\varepsilon_{572} = 54\ mM^{-1}\cdot cm^{-1}$ [37], in standard reaction mixture composed of 0.25 M sucrose, 50 mM Tris-Cl (pH 8.0), and 0.2 mM EDTA, supplemented with 5 μM rotenone (if indicated), horseradish peroxidase (HP, 2 units/ml), and bovine erythrocyte superoxide dismutase (SOD, 6 units/ml). Superoxide production was monitored as SOD-sensitive acetylated cytochrome *c* (10 μM) reduction at 550 nm ($\varepsilon_{550} = 20\ mM^{-1}\cdot cm^{-1}$) [38]. Increasing cytochrome *c* concentration up to 30 μM did not increase its SOD-sensitive reduction, but it did increase the SOD-insensitive reaction. SOD-insensitive components of acetylated cytochrome *c* reduction during aerobic oxidation of succinate or NADH were less than 25%. Addition of rotenone decreased the SOD-insensitive fraction of NADH-supported cytochrome *c* reduction to 5–7%. The amount of H_2O_2 determined by Amplex Red assay is the sum of the specifically produced H_2O_2 plus H_2O_2 resulting from dismutation (SOD-catalyzed and spontaneous) of two specifically produced superoxide radicals. We noted that some samples of HP display superoxide dismutase activity (intrinsic or due to contaminations), which might result in overestimation of the specific H_2O_2 production if both hydrogen peroxide and superoxide were the reaction products. Thus, the specific hydrogen peroxide-producing activity H_2O_2(specific) was calculated as follows:

$$H_2O_2(\text{specific}) = H_2O_2(\text{total}) - 2O_2^{\bullet}$$

where H_2O_2(total) is the amount of hydrogen peroxide assayed with Amplex Red in the presence of SOD, and $O_2^{\bullet}$ is the amount of superoxide determined as SOD-sensitive acetylated cytochrome *c* reduction. It has been shown that under certain conditions HP is capable of NADH oxidation-related ROS production in the process which is prevented by SOD [39]. Thus the experiments were conducted to assure that no undesired, catalyzed by any other than complex I preparation ROS production proceeded during the assays under the conditions employed. Fig. 1A demonstrates that no resorufin formation occurred during assay period unless total (superoxide plus hydrogen peroxide) ROS production was initiated by the addition of SMP. The reaction proceeded as zero-order process and the rates were calculated as the slope of actual tracings. When very low NADH concentrations were used, the registration curve deviated from linearity in time-dependent manner due to NADH decrease and NAD^+ increase. However, the initial slope of the actual registration curve could be easily determined if proper amount of the enzyme and time resolution scale were used. Fig. 1B shows analogous representative control experiments where SOD-sensitive acetylated cytochrome *c* reduction was assayed as a measure of complex I catalyzed superoxide production.

NADH:acceptor oxidoreductase activities were determined in the standard reaction mixture supplemented with the proper electron acceptor as a decrease in NADH absorption at 340 nm ($\varepsilon_{340} = 6.2\ mM^{-1}\cdot cm^{-1}$) or as a decrease in ferricyanide absorption at 420 nm ($\varepsilon_{420} = 1.0\ mM^{-1}\cdot cm^{-1}$). The specific activities are expressed as 2ē-equivalents, i.e. the amount of NADH oxidized. The results presented are average values of at least three independent assays.

Amplex Red was from AnaSpec, Inc. (U.S.A.); fine chemicals: nucleotides; trypsin (type XIII from bovine pancreas); trypsin inhibitor (type II-S from soybean); horseradish peroxidase (type II); SOD from bovine erythrocytes; partially acetylated cytochrome *c* from equine heart; alcohol dehydrogenase from bakers yeast; Q_1; and inhibitors were from Sigma-Aldrich (U.S.A.). Other chemicals of highest purity available were from local suppliers.

3. Results

3.1. Experimental system

Inside-out bovine heart SMP and complex I purified according to Hatefi's procedure were used throughout this study, and total hydrogen peroxide production in the presence of superoxide dismutase measured by Amplex Red assay or superoxide production measured as SOD-sensitive acetylated cytochrome *c* reduction were used to quantify the total and particular species of ROS. It has been shown that a considerable fraction of NADH-supported H_2O_2 formation by permeabilized heart mitochondria can be accounted for by hydrogen peroxide generation by DLDH located in matrix [7,8], hence it seemed worthwhile to determine whether SMP prepared by our routine procedure [34,35] contain any DLDH either as contamination or as intrinsic membrane-bound form of the enzyme. DLDH activity is known to be very sensitive to trypsinolysis [40], and tryptic digestion was used to detect possible presence of DLDH activity in our standard SMP. The data presented in Table 1 show that: (i) SMP indeed contain some lipoamide reductase activity, which was completely destroyed by controlled tryptic digestion; (ii) in the absence of activating ammonium [41], the contribution from DLDH to the NADH-supported hydrogen peroxide formation determined as the activity insensitive to NADH-OH, a specific inhibitor of complex I [42], was less than 10%; (iii) under the conditions employed (see Materials and methods section) tryptic digestion did not significantly affect complex I activity. Separate experiments showed that tryptic digestion resulted in a decrease in coupling efficiency. The respiratory control ratio with NADH as the substrate before and after trypsin treatment was 8.3 and 3.3, respectively. The data shown in Table 1 proved that the standard SMP as prepared in our laboratory are a simple and reliable system for studies on ROS production mediated by the respiratory chain

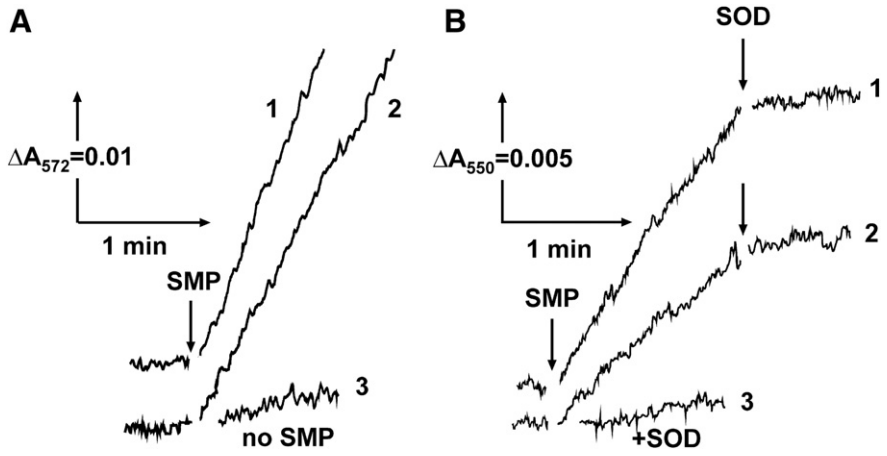

Fig. 1. Representative samples of the total hydrogen peroxide formation (A, Amplex Red assay) and superoxide generation (B, acetylated cytochrome *c* assay, SOD (6 units/ml) was added where indicated). The reactions were initiated by the addition of SMP (100 μg/ml, where indicated) to the standard reaction mixture. Curves 1 and 2, 50 and 500 μM NADH, respectively, were added to the assays. Curves 3: A, 500 μM NADH, SOD (6 units/ml), no SMP were added; B, SOD (6 units/ml) was present in the assay mixture before SMP addition. An increase of SOD amount did not change the pattern shown.

components only. Further experiments were done using the standard SMP (no treatment by trypsin).

3.2. H_2O_2 and $O_2^{\bullet-}$ generation by membrane-bound and purified complex I

The total NADH-supported ROS production catalyzed by rotenone-treated SMP at optimal (for superoxide generation) NADH concentration (50 μM) was about 4 nmol NADH oxidized/min per mg of protein, the activity corresponding to about 0.25% of their catalytic capacities in the respiratory chain-mediated NADH oxidase activity. The membrane-bound (SMP) and purified complex I were capable of both superoxide and hydrogen peroxide formation, and partitioning of either species was dependent on NADH concentration.

Fig. 2 summarizes the data on NADH dependence of superoxide and hydrogen peroxide production by SMP and purified complex I in the presence of rotenone, conditions where any reduced component of complex I could mediate one- or two-electron reduction of oxygen, except for bulk ubiquinol and N-2-associated semiquinones. The pattern shown in Fig. 2A (superoxide production) agrees with previously reported data [12] on inhibitory effect of high NADH concentrations, whereas essentially no inhibition was seen when hydrogen peroxide production was determined in the same concentration range of NADH (Fig. 2B). The data shown in Fig. 2, panels B and C, may appear contradictory: no hydrogen peroxide formation at NADH concentration below 3 μM is documented in panel C, whereas a hyperbola-like curve for the same activity is shown in panel B. This apparent inconsistency is clarified by the more detailed titration pattern for low NADH concentration range as shown in Fig. 3.

At low NADH (≤3 μM) only superoxide was produced, whereas more than 60% of the total reaction product appeared as hydrogen peroxide at higher (≥50 μM) NADH concentrations. The same pattern was seen for purified complex I (Fig. 2D) suggesting that under the conditions employed no other than complex I enzymes contributed to the overall ROS production by the SMP.

Complex I, an intrinsic component of the proton motive force-generating respiratory chain, is capable of rotenone- and uncoupler-inhibited ROS production when bulk ubiquinol provided by complex II during coupled succinate oxidation serves as the substrates for energy-dependent quinol:oxygen oxidoreduction [43] (energy-linked reverse electron transfer [44]). This reaction is of particular interest for studies on complex I-catalyzed ROS production because it proceeds under conditions where the active FMN-containing substrate-binding site of the enzyme is free of nucleotides. Table 2 shows relative contribution of the reaction products to ROS formation during coupled respiration with succinate and NADH. Both superoxide (about 65%) and hydrogen peroxide (about 35%) were produced during the reverse operation of complex I (line 1). An improvement in coupling efficiency by BSA significantly increased, as expected, total ROS production and, more interestingly, changed the proportion between the reaction products (line 2). Almost the same total ROS production was seen during succinate- (reverse) and NADH-supported (forward) operation of complex I (line 2 and 3). Rotenone stimulated the NADH-supported reaction and also increased the relative contribution of hydrogen peroxide. A general pattern emerging from the data shown in Table 2 is that the higher reduction level of complex I was reached the higher the rate of total ROS production was seen and the larger relative contribution of hydrogen peroxide was observed.

Table 1
Effect of tryptic digestion on catalytic activities of SMP.

	Activity (nmol/min per mg)[a] pH 8.0, 30 °C	
	Standard SMP	Trypsin-treated SMP
NADH-oxidase[b]	1600 ± 150	1450 ± 120
NADH:Q_1-reductase[c]	900 ± 70	850 ± 50
Lipoamide reductase[d]	50 ± 5	Undetectable
Total hydrogen peroxide formation[e]	4.0 ± 0.2	4.0 ± 0.15
+ NH_4Cl[f]	4.6 ± 0.3	3.7 ± 0.4
+ NADH-OH[g]	0.37 ± 0.05	0.27 ± 0.03
+ NADH-OH[g], + NH_4Cl[f]	1.85 ± 0.15	0.65 ± 0.07

[a] Averaged data from at least three assays performed with the same batch of SMP.
[b] NADH (100 μM) as the substrate, 0.2 μg/ml gramicidin D in the standard assay mixture.
[c] NADH (100 μM) and Q_1 (80 μM) as the substrates, 0.2 μg/ml gramicidin D and antimycin A (1 μg/ml) in the standard assay mixture.
[d] NADH (100 μM) and lipoamide (1 mM) as the substrates.
[e] In the presence of 100 μM NADH and 5 μM rotenone, assayed with Amplex Red.
[f] 30 mM NH_4Cl was added to the standard assay mixture
[g] Preincubated with NADH-OH (5 nmol per mg of protein) at 23 °C for 1 min before assay.

3.3. Redox titration of NADH-supported ROS generation

To gain further insight into quantitative aspects H_2O_2 and $O_2^{\bullet-}$ as the reaction product, the specific rates of generation of each species as a function of NAD^+/NADH ratio were measured (Fig. 4). The optimal (for superoxide production) concentration of (NAD^+ + NADH) pool (50 μM, see Fig. 2A) was used in the titration experiments. H_2O_2 production was significantly more sensitive to an increase in NAD^+/NADH ratio than that of superoxide formation: half-maximal rates of

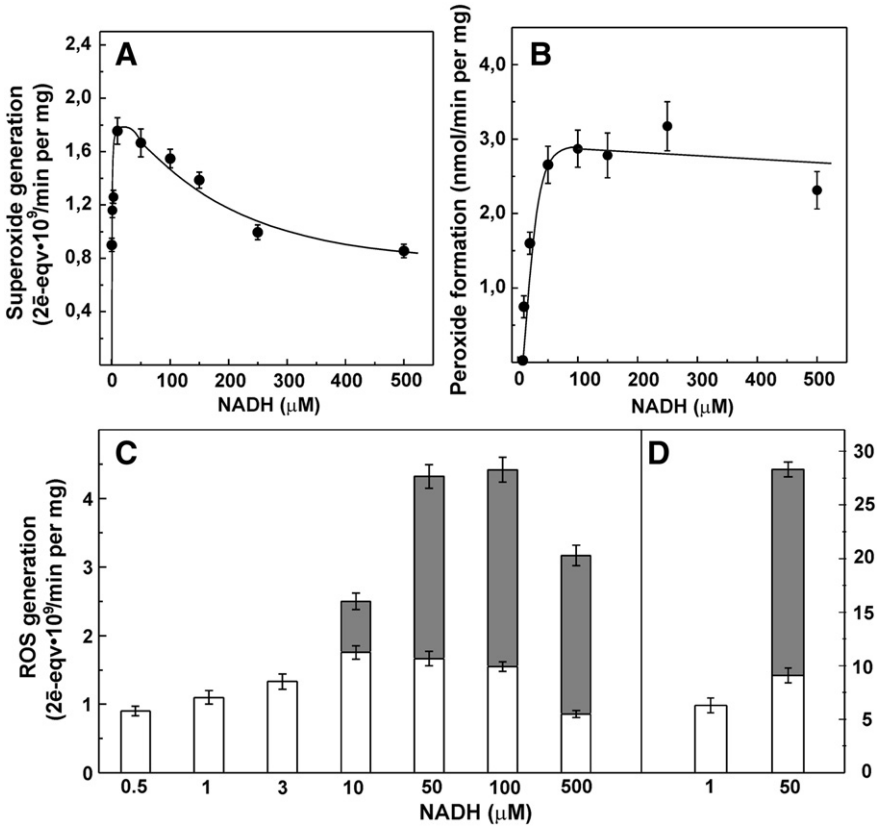

Fig. 2. NADH-supported superoxide and hydrogen peroxide production by the membrane-bound (A–C) and purified complex I (D) as a function of NADH concentration. All the activities were measured in the standard reaction mixture supplemented with 5 μM rotenone. A, superoxide generation measured as SOD-sensitive acetylated cytochrome *c* reduction. B, hydrogen peroxide production measured as the difference between total resorufin formed and superoxide determined as in A (see Materials and methods). C, contribution of superoxide (open bars) and hydrogen peroxide (gray bars) to the total ROS production. D, the same as C, ROS generation by purified complex I was determined as in A and B, respectively. The reactions were initiated by the additions of 100 (SMP, A–C) or 30 (complex I, D, right ordinate) μg of protein per ml of the assay mixture and the initial rates were measured.

hydrogen peroxide and superoxide were observed at NAD^+/NADH ratios of 0.13 and 0.33, respectively. The titration curve for H_2O_2 production satisfactory fitted the Nernst equation corresponding to apparent midpoint potential of a two-electron donor with midpoint potential of −347 mV (Fig. 4A, closed circles). The titration curve for superoxide production could not be fitted by the Nernst equation (Fig. 4B, closed circles). Note should be made that the data shown in Fig. 4 are certainly not classical redox titration curves. The dissociation constants for oxidized and reduced NAD binding to the oxidized and reduced enzyme are the parameters that, in addition to true redox equilibrium, determine the concentration of the enzyme capable of uni- or divalent reoxidation by oxygen. These binding constants were shown to be dependent on the reduction of the enzyme [45].

3.4. Effect of guanidine on complex I-mediated ROS production

We have claimed previously that guanidine increases NADH-supported superoxide production [12] similar to its stimulatory effect on the NADH:ferricyanide reductase activity [31,32]. This phenomenon was further investigated. Three-fold increase in NADH-supported

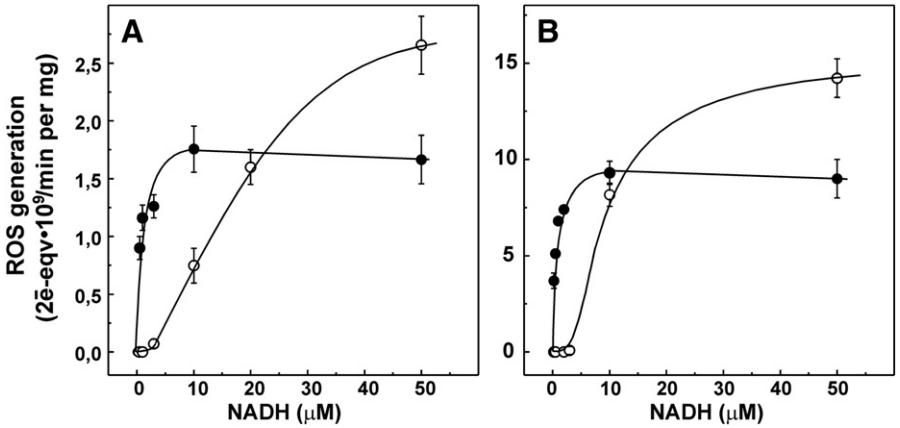

Fig. 3. NADH-supported superoxide and hydrogen peroxide production by membrane-bound (A) and purified complex I (B) at low NADH concentrations. Superoxide (●) and hydrogen peroxide production (○) were measured as in Fig. 2.

Table 2
Superoxide and hydrogen peroxide production by SMP during coupled NADH and succinate oxidation.

Substrate	Product formation rate[a] (2ē-eqv•10^9/min per mg of protein)			
	Superoxide (A)	Hydrogen peroxide (B)	A + B	A/B ratio
1. Succinate (5 mM)[b]	0.9 ± 0.1	0.5 ± 0.1	1.4 ± 0.1	1.90 ± 0.10
2. + BSA (1 mg/ml)[c]	1.0 ± 0.1	1.2 ± 0.2	2.2 ± 0.2	0.70 ± 0.15
NADH (50 μM)				
3. – rotenone	1.1 ± 0.1	1.2 ± 0.2	2.3 ± 0.2	0.85 ± 0.05
4. +5 μM rotenone	1.8 ± 0.2	2.8 ± 0.3	4.6 ± 0.3	0.65 ± 0.05

[a] Averaged data from at least three assays with the same batch of SMP.
[b] Rotenone-sensitive ROS production, i.e. complex I-catalyzed activities are documented. The succinate-supported, rotenone-insensitive activities (complex II + complex III contribution), 0.36 ± 0.06 (2ē-eqv•10^9/min per mg of protein), were subtracted from the actually observed rates of superoxide or hydrogen peroxide formation.
[c] BSA was added to increase coupling efficiency. The respiratory control ratio was 4.5 ± 0.5 and 7.8 ± 0.5 in the absence and presence of BSA, respectively.

superoxide production by complex I in SMP was observed at high (saturating) guanidine chloride concentration (Fig. 5A). An increase in ROS production depends hyperbolically on guanidine concentrations with half-maximal stimulation at 20 mM (results not shown). Three samples of guanidine chloride obtained from different suppliers showed identical effects. The stimulation was not due to the well-known general chaotropic properties of guanidine salts: guanidine isothiocyanate showed the same effect as did the chloride salt. A guanidine derivative, metformin, an antidiabetic drug that is known to inhibit complex I activity [46] at 50 mM concentration, showed only weak (1.4-fold) stimulation on the NADH-supported superoxide production catalyzed by the membrane-bound complex I (SMP) in the presence of rotenone.

Guanidine changed neither overall NADH oxidase nor NADH:quinone reductase activities, whereas it altered complex I reactivity with artificial electron acceptors and oxygen (Table 3). It inhibited NADH:HAR reductase and stimulated ferricyanide reduction and ROS production. The same stimulation (3-fold) of ferricyanide and oxygen univalent reduction was evident, whereas a smaller increase in H_2O_2 production (1.5-fold) was observed (Table 3 and Fig. 5). We were unable to evaluate the effect of guanidine on rotenone-sensitive succinate-supported ROS production (reverse electron transfer) because guanidine strongly inhibited aerobic succinate-supported NAD^+ reduction catalyzed by tightly coupled SMP. The latter phenomenon was, at least partially, due to the inhibitory effect of guanidine on succinate oxidase (Table 3, line 7).

Next the effect of guanidine on superoxide and hydrogen peroxide production by purified complex I at various NADH concentrations was tested (Fig. 6A–C). Both hydrogen peroxide and superoxide production were stimulated by guanidine. Only superoxide formation was analyzed by the standard kinetic approach, i.e. double-reciprocal plot constructed for very low concentrations of NADH (ascending parts of the curves shown in Fig. 6A). The linear dependencies shown in Fig. 6B suggest that guanidine increased the maximal rate without notable effect on apparent K_m^{NADH}. No such simple analysis could be done for hydrogen peroxide formation because the dependence on NADH was not hyperbolic, as is shown in Fig. 3.

Finally, the effect of guanidine on the redox dependence of ROS production was assessed (Fig. 4, A and B, open symbols). Guanidine shifted the redox titration curves for both superoxide and hydrogen peroxide formation to more positive apparent redox potentials. Half-maximal rates of ROS production in the presence of guanidine were at NAD^+/NADH ratios of 0.42 for H_2O_2 and 2.54 for $O_2^{\bullet}$ production versus 0.13 for H_2O_2 and 0.33 for $O_2^{\bullet}$ production in the absence of guanidine.

4. Discussion

4.1. Experimental system

The specific activities reported in numerous publications on the mitochondrial ROS production determined either on protein or particular component content basis are highly variable. Besides natural species and tissue specificity [47–49], the type of preparation used for the assays seems to be important. Several experimental systems for studies of ROS generation by complex I are available. Isolated mitochondria generate H_2O_2 in State 4, i.e. under conditions when the intramitochondrial pyridine nucleotide pool is highly reduced. Quantitative analysis of complex I-mediated superoxide and hydrogen peroxide production by intact mitochondria is hampered by the presence of glutathione reductase, glutaredoxins, glutathione peroxidase system, and

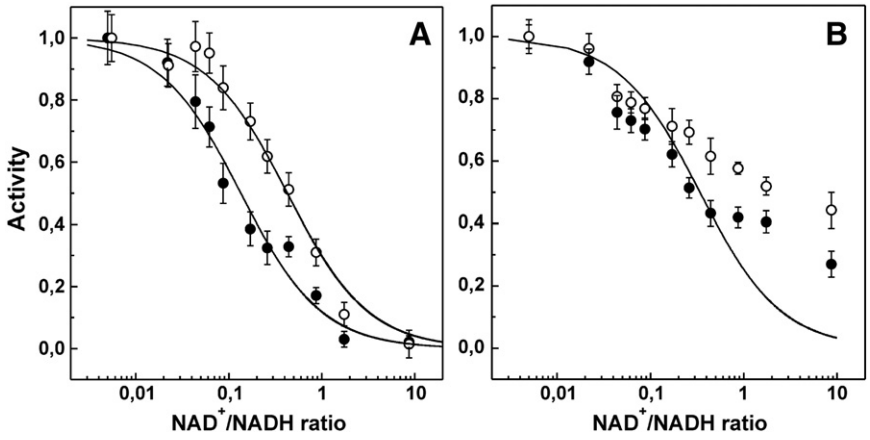

Fig. 4. NADH-supported ROS production by SMP as a function of NAD^+/NADH ratio. Hydrogen peroxide (A) and superoxide production (B) were measured as in Fig. 2 at 50 μM pool of (NAD^+ + NADH) in the absence (●) and in the presence (○) of 50 mM guanidine chloride. Continuous lines, theoretical curves corresponding to the Nernst equation for two-electron reactive redox components equilibrated with ambient midpoint potentials set by NAD^+/NADH ratio equal to: A, ~347 mV (closed symbols), -331 mV (open symbols), and B, -334 mV. The activities were normalized to those observed in the absence of NAD^+. The additions of 100 mM ethanol and alcohol dehydrogenase (250 units/ml) did not change normalized activities.

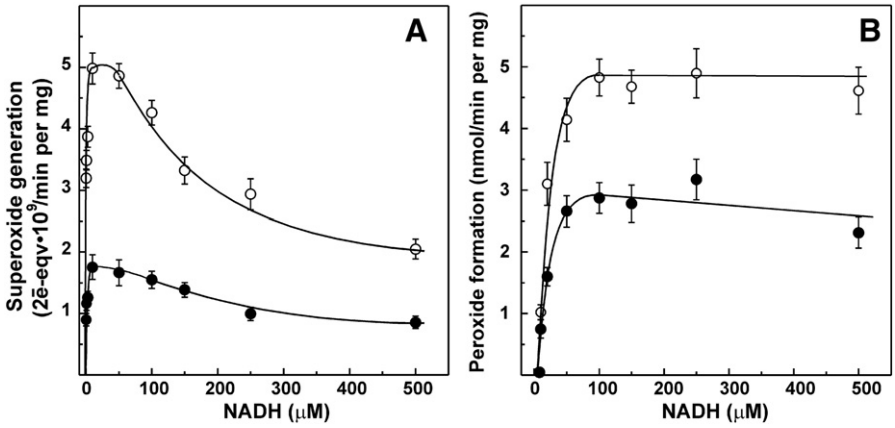

Fig. 5. Effect of guanidine chloride on superoxide (A) and hydrogen peroxide production (B) by SMP. The specific activities were determined as in Fig. 2 in the absence (●) and in the presence (○) of 50 mM guanidine chloride.

catalase in the matrix space [50,51]. Also, as noted above, matrix located dehydrogenases, particularly DLDH [7,9–11], significantly contribute to the overall mitochondrial ROS production. Purified preparations of complex I [36,52,53] seem much better suited for studies on its catalytic, particularly ROS-generating activity. However, no simple techniques are available to impose proton motive force for simulation of "physiologically" relevant conditions when purified detergent-dispersed complexes I are used. Also, the detergents used for purification of complex I may alter its catalytic activities [54,55]. To compromise between extremely complex (mitochondria) and simplest well defined (purified complex I) experimental systems, inside-out coupled SMP [34,35] are routinely used in our studies on complex I. Here we showed that our "standard" SMP retain some DLDH activity (Table 1), despite extensive dilution, washing, and Sephadex column filtration during the preparation. This finding is indicative of the presence of membrane-bound DLDH in mitochondria. SMP-bound hydrogen peroxide generating activity was increased 5-fold by ammonium (Table 1), this being qualitatively similar to the phenomenon previously described for the soluble enzyme [11,41]. Whether other properties of the membrane-bound DLDH are the same as those of free soluble protein remains to be established. SMP completely devoid of DLDH activity can be easily prepared (Table 1) and used for DLDH reconstitution studies, which are currently underway in our laboratory. In the absence of activating ammonium, the contribution of other than complex I generating sources to the overall production catalyzed by either standard or trypsin-treated SMP was less than 10% as evident from 90% inhibition by complex I-specific NADH-OH (Table 1).

Table 3
Effect of guanidine chloride on SMP activities.

	Activity, (2ē-eqv•10^9/min per mg) pH 8.0, 30 °C		
	control (A)	+50 mM guanidine chloride (B)	B/A
1. NADH-oxidase[a]	1650±130	1640±140	0.9
2. NADH:Q_1-reductase[a]	900±70	810±50	0.9
3. NADH:HAR-reductase[b]	2600±130	1900±70	0.7
4. NADH: ferricyanide-reductase[c]	4100±500	12500±1500	3.0
5. Superoxide formation[d]	1.8±0.1	5.0±0.2	2.8
6. Hydrogen peroxide formation[d]	2.7±0.2	4.1±0.2	1.5
7. Succinate oxidase[e]	830±70	580±50	0.7

[a] Assayed and average as described in Table 1.
[b] NADH (100 μM) and HAR (0.5 mM) as the substrates, 5 μM rotenone in the standard assay mixture.
[c] NADH (100 μM) and ferricyanide (0.5 mM) as the substrates, 5 μM rotenone in the standard assay mixture.
[d] NADH (50 μM) as the substrate, 5 μM rotenone in the standard assay mixture.
[e] Potassium succinate (5 mM) as the substrate, 0.2 μg/ml gramicidin D in the standard assay mixture.

4.2. Hydrogen peroxide and superoxide generation by complex I

Both, H_2O_2 and $O_2^{\bullet-}$ are produced by complex I, and the partitioning of the reaction products depends on NADH concentration (Fig. 2). Only superoxide was generated by the membrane-bound and purified complex I at low NADH (1–3 μM) in a reaction with apparent K_m^{NADH} of 0.5 μM (data for purified complex I, Fig. 6B), a value that is significantly higher than that (0.05 μM, at pH 7.5, 32 °C) reported for superoxide production by bovine heart complex I purified by a different isolation procedure [24]. Since the rate of ROS production by complex I is much slower than the enzyme capacity in reactions with electron acceptors other than oxygen, it is safe to assume that all its redox components are in true equilibrium during steady-state NADH:oxygen oxidoreduction. The apparent K_m for the substrate-electron donor in the reaction catalyzed by any oxidoreductase that contain several linearly arranged redox components depends on thermodynamic gap between the primary electron acceptor and the component reacting with the substrate-oxidant; the larger the gap is, the lower K_m is expected to be [56]. Very low apparent K_m^{NADH} in ROS generation [24, this paper] as compared with those reported for reactions with other artificial electron acceptors [43] suggests that a component with significantly more positive potential than that of the primary acceptor (FMN) is the actual donor for one-electron reduction of oxygen. The data on the redox titration of superoxide production (Fig. 4B) show that a substantial rate (about 20% of the maximal) was observed at NAD^+/NADH ratio as high as 10:1, corresponding to the ambient redox potential of −290 mV at pH 8.0. This value is much higher than that for the FMN/FMN^- couple (about −370 mV at pH 8.0) in complex I [33]. At present, we are unable to unambiguously identify a component responsible for superoxide production. The iron–sulfur center N-2 seems to be a likely candidate in light of the large thermodynamic gap between the primary electron acceptor (FMN) and the final electron donor (see above). An obvious question arises: what is the explanation for the inhibitory effect of high NADH concentrations on superoxide production if the iron–sulfur cluster located far away from NADH binding site [16,17] is the electron donor? It has been shown recently that eukaryotic complexes I bear an allosteric nucleotide (ATP)-binding site that, when filled, strongly stimulates NADH:HAR reductase activity [57]. We hypothesized that binding of ATP at this site modulates the redox potential of iron–sulfur center N-2 and/or its accessibility for HAR [57] (see a different interpretation of the phenomenon in Ref. [58]). The stimulatory effect of ATP is completely eliminated by increased concentration of NADH, thus suggesting that NADH can bind to complex I at a site different from its conventional "substrate-

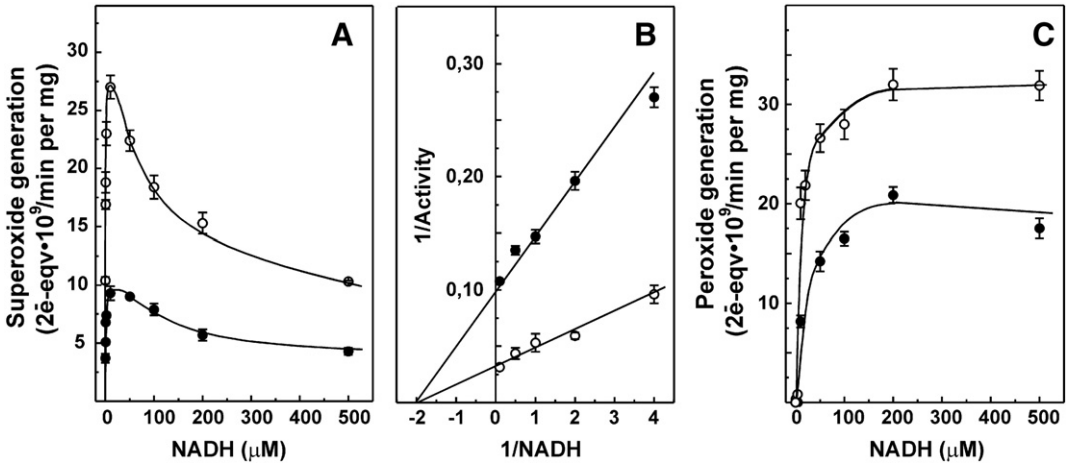

Fig. 6. Effect of guanidine chloride on superoxide (A and B) and hydrogen peroxide production (C) by purified complex I. The specific activities were determined as in Fig. 2 in the absence (●) and in the presence (○) of 50 mM guanidine chloride. B, double reciprocal plot for ascending part of the curves shown in A (low concentrations of NADH).

binding site". Filling of this "allosteric site" by NADH may alter the redox potential and/or accessibility of N-2 to oxygen. Interestingly, ferricyanide reductase activity of *Paracoccus denitrificans* NDH-1, a prokaryotic homolog of complex I that is devoid of the allosteric nucleotide binding site [57], shows only weak inhibition by NADH [59]. The proposal on center N-2 as the source of superoxide is in apparent contradiction with the data of Galkin and Brandt, who have shown that a mutation of *Yarrowia lipolytica* complex I that eliminated the N-2 EPR signal did not inhibit its superoxide generating activity [60]. It should be noted that the mutation may make N-2 EPR-silent though still capable of oxygen reactivity. Also, other than N-2 iron–sulfur center(s), except, perhaps, N-1a with much lower midpoint redox potential [61], can be considered as the potential source of superoxide following the reasoning discussed above.

The kinetics and "thermodynamics" of hydrogen peroxide generation were different from those of superoxide production. The difference can be summarized as follows. (i) H_2O_2 is formed at substantially higher NADH concentrations, and sigmoidal dependence on the substrate concentration is evident (Fig. 3) with half-maximal activity at 25 μM (compare with apparent K_m^{NADH} of 0.5 μM in superoxide production in Fig. 6B). (ii) In contrast to superoxide, hydrogen peroxide generation is essentially insensitive to high NADH concentration. This finding agrees poorly with the proposed explanation of the inhibitory effect of NADH on ROS production as shielding of the enzyme reactive center (presumably $FMNH^-$) by bound nucleotide, thus decreasing its oxygen accessibility [62]. (iii) The redox titration of NADH-supported H_2O_2 production (Fig. 4A) is well fitted to a Nernst equation for a two-electron/one proton oxidoreduction with ambient (NAD^+/NADH) midpoint potential of −347 mV at pH 8.0, a value substantially more negative than that for superoxide production (Fig. 4B).

It should be noted that $FMNH^-$ was suggested as the site of superoxide, not hydrogen peroxide, production by the bovine heart complex I purified by an alternative procedure [52]. This proposal was based on the redox profile of superoxide generation fitted to the Nernst equation with ambient (NAD^+/NADH) midpoint potential of approximately −360 mV at pH 8.0 (see Fig. 5 in Ref [24]). Also, it has been noted, in apparent contradiction with the data reported here, that purified bovine heart complex I generates 95% ROS as superoxide, whereas *E. coli* NDH-1, the prokaryotic homolog of complex I, produces 20% $O_2^{\bullet}$ and 80% H_2O_2 during NADH-supported ROS generation [63]. The reasons for different results reported here and those obtained by others are not clear. Different experimental systems were used: bovine heart SMP and traditional complex I (this paper) and detergent-dispersed pure complex I [24] and SMP [25] prepared by an alternative procedure. Another, perhaps more significant, difference is that ROS production by SMP only at low concentration of NADH (30 μM) was analyzed by Pryde and Hirst [25], whereas partitioning of the products depends on NADH concentration (Fig. 2C and D).

Both superoxide and hydrogen peroxide productions are sensitive to NAD^+ [12] and NAD^+/NADH ratio ([8,22,24,25,27] and this paper). On the other hand, NADH oxidase activity catalyzed by complex I is only weakly inhibited (competitively) by NAD^+ ($K_i^{NAD^+}$ is in millimolar range [43]). A plausible explanation for this apparent discrepancy most likely rests upon overall kinetics of NADH:ubiquinone reduction in the respiratory chain catalyzed by complex I. Reoxidation of iron–sulfur center N-2 is evidently the rate-limiting step during the coupled or uncoupled steady-state NADH oxidase reaction [21,35]. As expected from the redox gap between the FMN/$FMNH^-$ and $N\text{-}2_{ox}/N\text{-}2_{red}$ couples, the N-2 center remains mostly in the reduced form even when FMN is substantially oxidized (by the NAD^+/NADH couple), and the activities where $FMNH^-$ directly participates are inhibited.

In summary, we interpret our data on ROS production by complex I either in forward or reverse electron transfer as the presence of at least two different sites directly reacting with oxygen in complex I located upstream of the rotenone sensitive site: Site 1, most likely fully reduced FMN where oxygen reduction via a two-electron mechanism results in hydrogen peroxide formation, and Site 2, one of the iron–sulfur centers, most likely N-2, where one-electron reduction results in superoxide production.

Short note concerning physiological relevance of the data reported worth noting. The concentration of NADH required for half-maximal ROS production (0.5 μM and 25 μM for superoxide and hydrogen peroxide, respectively) are well below the physiologically relevant values. An average content of NADH + NAD^+ in heart mitochondria is in a range of 5–7 nmol/mg of protein [64–66], the values corresponding to 5–7 mM concentration in matrix (assuming 1 mg of protein corresponds to approximately 1 μl of water [67,68]). Although substantial part of this nucleotide pool may be bound to matrix located dehydrogenase it seems certain that complex I in intact mitochondria is always saturated by either NADH or NAD^+. Since superoxide production is inhibited by high physiologically relevant concentrations of NADH and/or NAD^+ ([12], this paper), hydrogen peroxide is expected to be the predominant species of ROS generated by complex I.

4.3. Stimulation of ROS production by guanidine

Guanidine has long been known to modulate catalytic activities of complex I [31,32]. In this study, we confirmed the opposite effects of guanidine on HAR (inhibition) and ferricyanide (activation) reductase

activities catalyzed by membrane-bound complex I (Table 3), whereas no significant effects on other major catalytic activities, NADH oxidase and quinone reductase, were found. Both superoxide and hydrogen peroxide production by complex I was activated by guanidine (Table 3). Only the maximal rate was increased with no change in K_m^{NADH} when the superoxide production rate hyperbolic dependence on NADH was measured (Fig. 6B). The redox titration curve in the presence of guanidine was shifted to more positive ambient redox potential set up by NAD^+/NADH ratio for hydrogen peroxide (Fig. 4A and B). This can be interpreted as an increase in the redox potential of the FMN/$FMNH^-$ couple resulting from interaction of reduced flavin anion with guanidine cation, as discussed by Sled et al. [33], assuming that $FMNH^-$ is the electron donor for hydrogen peroxide production. The stimulatory effect of guanidine on ferricyanide reduction can be explained by an increase in semiquinone fraction observed upon redox titration of complex I [33] if flavin semiquinone participates during the steady-state ferricyanide reduction.

Direct interaction of oxygen with complex I is likely a "leakage" reaction, so no specific channels created during evolution to facilitate the accessibility of the enzyme redox component to oxygen exist in the protein structure, in contrast to true oxidases [69,70] or oxygen carrying proteins [71,72]. The existence of at least two leakage "sites" producing different products (H_2O_2 and $O_2^{\bullet}$) as evident from the data reported here is not unexpected. Accumulated evidence strongly suggest that FMN is one such site. The reduction of flavin in a FP fragment [73] and in membrane-bound complex I [74] results in drastic change of its binding to the protein, leading to dissociation if the system is properly diluted. Redox-dependent rearrangement of FMN may serve as a driving force for long-distance conformational change of the entire structure of complex I that would change accessibility of iron–sulfur clusters for oxygen that diffuses through the protein. The conformational flexibility of complex I structure is well documented [75–77].

Acknowledgements

This study was supported by grant 11-04-00916 to ADV and grant 12-04-00602 to VGG of the Russian Foundation for Fundamental Research.

References

[1] A. Boveris, N. Oshino, B. Chance, The cellular production of hydrogen peroxide, Biochem. J. 128 (1972) 617–630.
[2] G. Loschen, L. Flohé, B. Chance, Respiratory chain linked H_2O_2 production in pigeon heart mitochondria, FEBS Lett. 18 (1971) 261–264.
[3] T.V. Votyakova, I.J. Reynolds, $\Delta\Psi_m$-dependent and -independent production of reactive oxygen species by rat brain mitochondria, J. Neurochem. 79 (2001) 266–277.
[4] B. Chance, H. Sies, A. Boveris, Hydroperoxide metabolism in mammalian organs, Physiol. Rev. 59 (1979) 527–605.
[5] I. Fridovich, Mitochondria: are they the seat of senescence? Aging Cell 3 (2004) 13–16.
[6] A.A. Starkov, The role of mitochondria in reactive oxygen species metabolism and signaling, Ann. N. Y. Acad. Sci. 1147 (2008) 37–52.
[7] V.G. Grivennikova, A.V. Kareyeva, A.D. Vinogradov, What are the sources of hydrogen peroxide production by heart mitochondria? Biochim. Biophys. Acta 1797 (2010) 939–944.
[8] A.V. Kareyeva, V.G. Grivennikova, A.D. Vinogradov, Mitochondrial hydrogen peroxide production as determined by the pyridine nucleotide pool and its redox state, Biochim. Biophys. Acta 1817 (2012) 1879–1885.
[9] A.A. Starkov, G. Fiskum, C. Chinopoulos, B.J. Lorenzo, S.E. Browne, M.S. Patel, M.F. Beal, Mitochondrial alpha-ketoglutarate dehydrogenase complex generates reactive oxygen species, J. Neurosci. 24 (2004) 7779–7788.
[10] L. Tretter, V. Adam-Vizi, Generation of reactive oxygen species in the reaction catalyzed by α-ketoglutarate dehydrogenase, J. Neurosci. 24 (2004) 7771–7778.
[11] A.V. Kareyeva, V.G. Grivennikova, G. Cecchini, A.D. Vinogradov, Molecular identification of the enzyme responsible for the mitochondrial NADH-supported ammonium-dependent hydrogen peroxide production, FEBS Lett. 585 (2011) 385–389.
[12] V.G. Grivennikova, A.D. Vinogradov, Generation of superoxide by the mitochondrial Complex I, Biochim. Biophys. Acta 1757 (2006) 553–561.
[13] J. Carroll, I.M. Fearnley, J.M. Skehel, R.J. Shannon, J. Hirst, J.E. Walker, Bovine Complex I is a complex of 45 different subunits, J. Biol. Chem. 281 (2006) 32724–32727.
[14] E. Balsa, R. Marco, E. Perales-Clemente, R. Szklarczyk, E. Calvo, M.O. Landázuri, J.A. Enríquez, NDUFA4 is a subunit of complex IV of the mammalian electron transport chain, Cell Metab. 16 (2012) 378–386.
[15] U. Brandt, Energy converting NADH:quinone oxidoreductase (complex I), Annu. Rev. Biochem. 75 (2006) 69–92.
[16] L.A. Sazanov, Respiratory complex I: mechanistic and structural insights provided by the crystal structure of the hydrophilic domain, Biochemistry 46 (2007) 2275–2288.
[17] R.G. Efremov, R. Baradaran, L.A. Sazanov, The architecture of respiratory complex I, Nature 465 (2010) 441–445.
[18] B. Halliwell, Reactive oxygen species and the central nervous system, J. Neurochem. 59 (1992) 1609–1623.
[19] D. Harman, The free radical theory of aging, Antioxid. Redox Signal. 5 (2003) 557–561.
[20] R.S. Balaban, S. Nemoto, T. Finkel, Mitochondria, oxidants, and aging, Cell 120 (2005) 483–495.
[21] A.I.G. Krishnamoorthy, P. Hinkle, Studies on the electron transfer pathway, topography of iron–sulfur centers, and site of coupling in NADH-Q oxidoreductase, J. Biol. Chem. 263 (1988) 17566–17575.
[22] A.P. Kudin, N.Y. Bimpong-Buta, S. Vielhaber, C.E. Elger, W.S. Kunz, Characterization of superoxide-producing sites in isolated brain mitochondria, J. Biol. Chem. 279 (2004) 4127–4135.
[23] A.D. Vinogradov, V.G. Grivennikova, Generation of superoxide-radical by the NADH:ubiquinone oxidoreductase of heart mitochondria, Biochem. Mosc. 70 (2005) 120–127.
[24] L. Kussmaul, J. Hirst, The mechanism of superoxide production by NADH:ubiquinone oxidoreductase (complex I) from bovine heart mitochondria, Proc. Natl. Acad. Sci. U. S. A. 103 (2006) 7607–7612.
[25] K.R. Pryde, J. Hirst, Superoxide is produced by the reduced flavin in mitochondrial complex I: a single, unified mechanism that applies during both forward and reverse electron transfer, J. Biol. Chem. 286 (2011) 18056–18065.
[26] S.T. Ohnishi, T. Ohnishi, S. Muranaka, H. Fujita, H. Kimura, K. Uemura, K. Yoshida, K. Utsumi, A possible site of superoxide generation in the complex I segment of rat heart mitochondria, J. Bioenerg. Biomembr. 37 (2005) 1–15.
[27] Y. Kushnareva, A.N. Murphy, A. Andreyev, Complex I-mediated reactive oxygen species generation: modulation by cytochrome c and $NAD(P)^+$ oxidation-reduction state, Biochem. J. 368 (2002) 545–553.
[28] M.L. Genova, B. Ventura, G. Giuliano, C. Bovina, G. Formiggini, G.P. Castelli, G. Lenaz, The site of production of superoxide radical in mitochondrial Complex I is not a bound ubisemiquinone but presumably iron–sulfur cluster N2, FEBS Lett. 505 (2001) 364–368.
[29] J.R. Treberg, C.L. Quinlan, M.D. Brand, Evidence for two sites of superoxide production by mitochondrial NADH-ubiquinone oxidoreductase (complex I), J. Biol. Chem. 286 (2011) 27103–27110.
[30] S.T. Ohnishi, K. Shinzawa-Itoh, K. Ohta, S. Yoshikawa, T. Ohnishi, New insights into the superoxide generation sites in bovine heart NADH:ubiquinone oxidoreductase (Complex I): the significance of protein-associated ubiquinone and dynamic shifting of generation sites between semiflavin and semiquinone radicals, Biochim. Biophys. Acta 1797 (2010) 1901–1909.
[31] Y. Hatefi, K.E. Stempel, W.G. Hanstein, Inhibitors and activators of the mitochondrial reduced diphosphopyridine nucleotide dehydrogenase, J. Biol. Chem. 244 (1969) 2358–2365.
[32] Y. Hatefi, Y.M. Galante, Dehydrogenase and transhydrogenase properties of the soluble NADH dehydrogenase of bovine heart mitochondria, Proc. Natl. Acad. Sci. U. S. A. 74 (1977) 846–850.
[33] V.D. Sled, N.I. Rudnitzky, Y. Hatefi, T. Ohnishi, Thermodynamic analysis of flavin in mitochondrial NADH:ubiquinone oxidoreductase (complex I), Biochemistry 33 (1994) 10069–10075.
[34] A.B. Kotlyar, A.D. Vinogradov, Slow active/inactive transition of the mitochondrial NADH-ubiquinone reductase, Biochim. Biophys. Acta 1019 (1990) 151–158.
[35] D.S. Burbaev, I.A. Moroz, A.B. Kotlyar, V.D. Sled, A.D. Vinogradov, Ubisemiquinone in the NADH-ubiquinone reductase region of the mitochondrial respiratory chain, FEBS Lett. 254 (1989) 47–51.
[36] Y. Hatefi, Preparation and properties of NADH: ubiquinone oxidoreductase (complex I), Methods Enzymol. 53 (1978) 11–14.
[37] M. Zhou, Z. Diwu, N. Panchuk-Voloshina, R.P. Haugland, A stable nonfluorescent derivative of resorufin for the fluorometric determination of trace hydrogen peroxide: applications in detecting the activity of phagocyte NADPH oxidase and other oxidases, Anal. Biochem. 253 (1997) 162–168.
[38] A. Azzi, C. Montecucco, C. Richter, The use of acetylated ferricytochrome c for the detection of superoxide radicals produced in biological membranes, Biochem. Biophys. Res. Commun. 65 (1975) 597–603.
[39] T.V. Votyakova, I.J. Reynolds, Detection of hydrogen peroxide with Amplex Red: interference by NADH and reduced glutathione auto-oxidation, Arch. Biochem. Biophys. 431 (2004) 138–144.
[40] R.L. Searls, D.R. Sanadi, α-Ketoglutaric dehydrogenase. VIII. Isolation and some properties of a flavoprotein component, J. Biol. Chem. 235 (1960) 2485–2491.
[41] V.G. Grivennikova, G. Cecchini, A.D. Vinogradov, Ammonium-dependent hydrogen peroxide production by mitochondria, FEBS Lett. 583 (2008) 1287–1291.
[42] A.B. Kotlyar, J.S. Karliner, G. Cecchini, A novel strong competitive inhibitor of complex I, FEBS Lett. 579 (2005) 4861–4866.
[43] A.D. Vinogradov, Catalytic properties of the mitochondrial NADH-ubiquinone oxidoreductase (complex I) and the pseudo-reversible active/inactive enzyme transition, Biochim. Biophys. Acta 1364 (1998) 169–185.
[44] B. Chance, G. Hollunger, Energy-linked reduction of mitochondrial pyridine nucleotide, Nature 185 (1960) 666–672.

[45] V.G. Grivennikova, A.B. Kotlyar, J.S. Karliner, G. Cecchini, A.D. Vinogradov, Redox-dependent change of nucleotide affinity to the active site of the mammalian complex I, Biochemistry 46 (2007) 10971–10978.
[46] M.R. Owen, E. Doran, A.P. Halestrap, Evidence that metformin exerts its anti-diabetic effects through inhibition of complex 1 of the mitochondrial respiratory chain, Biochem. J. 348 (2000) 607–614.
[47] E.B. Tahara, F.D. Navarete, A.J. Kowaltowski, Tissue-, substrate-, and site-specific characteristics of mitochondrial reactive oxygen species generation, Free Radic. Biol. Med. 46 (2009) 1283–1297.
[48] A.J. Lambert, H.M. Boysen, J.A. Buckingham, T. Yang, A. Podlutsky, S.N. Austad, T.H. Kunz, R. Buffenstein, M.D. Brand, Low rates of hydrogen peroxide production by isolated heart mitochondria associate with long maximum lifespan in vertebrate homeotherms, Aging Cell 6 (2007) 607–618.
[49] H.H. Ku, U.T. Brunk, R.S. Sohal, Relationship between mitochondrial superoxide and hydrogen peroxide production and longevity of mammalian species, Free Radic. Biol. Med. 15 (1993) 621–627.
[50] F. Antunes, D. Han, E. Cadenas, Relative contributions of heart mitochondria glutathione peroxidase and catalase to H_2O_2 detoxification in in vivo conditions, Free Radic. Biol. Med. 33 (2002) 1260–1267.
[51] A.G. Cox, C.C. Winterbourn, M.B. Hampton, Mitochondrial peroxiredoxin involvement in antioxidant defence and redox signaling, Biochem. J. 425 (2010) 313–325.
[52] M.S. Sharpley, R.J. Shannon, F. Draghi, J. Hirst, Interactions between phospholipids and NADH:ubiquinone oxidoreductase (complex I) from bovine mitochondria, Biochemistry 45 (2006) 241–248.
[53] K. Shinzawa-Itoh, J. Seiyama, H. Terada, R. Nakatsubo, K. Naoki, Y. Nakashima, S. Yoshikawa, Bovine heart NADH-ubiquinone oxidoreductase contains one molecule of ubiquinone with ten isoprene units as one of the cofactors, Biochemistry 49 (2010) 487–492.
[54] A.V. Ushakova, V.G. Grivennikova, T. Ohnishi, A.D. Vinogradov, Triton X-100 as a specific inhibitor of the mammalian NADH-ubiquinone oxidoreductase (Complex I), Biochim. Biophys. Acta 1409 (1999) 143–153.
[55] J.G. Okun, V. Zickermann, K. Zwicker, H. Schägger, U. Brandt, Binding of detergents and inhibitors to bovine complex I - a novel purification procedure for bovine complex I retaining full inhibitor sensitivity, Biochim. Biophys. Acta 1459 (2000) 77–87.
[56] A.D. Vinogradov, NADH/NAD^+ interaction with NADH: ubiquinone oxidoreductase (complex I), Biochim. Biophys. Acta 1777 (2008) 729–734.
[57] V.G. Grivennikova, G.V. Gladyshev, A.D. Vinogradov, Allosteric nucleotide-binding site in the mitochondrial NADH:ubiquinone oxidoreductase (respiratory complex I), FEBS Lett. 585 (2011) 2212–2216.
[58] J.A. Birrell, M.S. King, J. Hirst, A ternary mechanism for NADH oxidation by positively charged electron acceptors, catalyzed at the flavin site in respiratory complex I, FEBS Lett. 585 (2011) 2318–2322.
[59] V. Zickermann, S. Kurki, M. Kervinen, I. Hassinen, M. Finel, The NADH oxidation domain of complex I: do bacterial and mitochondrial enzymes catalyze ferricyanide reduction similarly? Biochim. Biophys. Acta 1459 (2000) 61–68.
[60] A. Galkin, U. Brandt, Superoxide radical formation by pure complex I (NADH: ubiquinone oxidoreductase) from *Yarrowia lipolytica*, J. Biol. Chem. 280 (2005) 30129–30135.
[61] T. Ohnishi, H. Blum, Y.M. Galante, Y. Hatefi, Iron–sulfur N-1 clusters studied in NADH-ubiquinone oxidoreductase and in soluble NADH dehydrogenase, J. Biol. Chem. 256 (1981) 9216–9220.
[62] J.M. Berrisford, L.A. Sazanov, Structural basis for the mechanism of respiratory complex I, J. Biol. Chem. 284 (2009) 29773–29783.
[63] D. Esterházy, M.S. King, G. Yakovlev, J. Hirst, Production of reactive oxygen species by complex I (NADH:ubiquinone oxidoreductase) from *Escherichia coli* and comparison to the enzyme from mitochondria, Biochemistry 47 (2008) 3964–3971.
[64] R.L. Lester, Y. Hatefi, Studies on the mechanism of oxidative phosphorylation. IV. Pyridine nucleotide binding and its relation to activity in heart mitochondria, Biochim. Biophys. Acta 29 (1958) 103–112.
[65] M. Klingenberg, W. Slenczka, E. Ritt, Vergleichende biochemie der pyridinnucleotid-systeme in mitochondrien verschiedener organe, Biochem. Z. (FEBS J.) 332 (1959) 47–66.
[66] Y. Avi-Dor, J.M. Olson, M.D. Doherty, N.O. Kaplan, Fluorescence of pyridine nucleotides in mitochondria, J. Biol. Chem. 237 (1962) 2377–2383.
[67] E.J. Harris, K. van Dam, Changes of total water and sucrose space accompanying induced ion uptake or phosphate swelling of rat liver mitochondria, Biochem. J. 106 (1968) 759–766.
[68] A.P. Halestrap, P.T. Quinlan, The intramitochondrial volume measured using sucrose as an extramitochondrial marker overestimates the true matrix volume determined with mannitol, Biochem. J. 214 (1983) 387–393.
[69] S. Riistama, A. Puustinen, A. García-Horsman, S. Iwata, H. Michel, M. Wikström, Channelling of dioxygen into the respiratory enzyme, Biochim. Biophys. Acta 1275 (1996) 1–4.
[70] R. Coulombe, K.Q. Yue, S. Ghisla, A. Vrielink, Oxygen access to the active site of cholesterol oxidase through a narrow channel is gated by an Arg–Glu pair, J. Biol. Chem. 276 (2001) 30435–30441.
[71] M. Brunori, D. Bourgeois, B. Vallone, The structural dynamics of myoglobin, J. Struct. Biol. 147 (2004) 223–234.
[72] M.D. Salter, G.C. Blouin, J. Soman, E.W. Singleton, S. Dewilde, L. Moens, A. Pesce, M. Nardini, M. Bolognesi, J.S. Olson, Determination of ligand pathways in globins: apolar tunnels versus polar gates, J. Biol. Chem. 287 (2012) 33163–33178.
[73] V.D. Sled, A.D. Vinogradov, Reductive inactivation of the mitochondrial three subunit NADH dehydrogenase, Biochim. Biophys. Acta 1143 (1993) 199–203.
[74] I.S. Gostimskaya, V.G. Grivennikova, G. Cecchini, A.D. Vinogradov, Reversible dissociation of flavin mononucleotide from the mammalian membrane-bound NADH: ubiquinone oxidoreductase (complex I), FEBS Lett. 581 (2007) 5803–5806.
[75] M. Radermacher, T. Ruiz, T. Clason, S. Benjamin, U. Brandt, V. Zickermann, The three-dimensional structure of complex I from *Yarrowia lipolytica*: a highly dynamic enzyme, J. Struct. Biol. 154 (2006) 269–279.
[76] A.A. Mamedova, P.J. Holt, J. Carroll, L.A. Sazanov, Substrate-induced conformational change in bacterial complex I, J. Biol. Chem. 279 (2004) 23830–23836.
[77] R. Hielscher, T. Friedrich, P. Hellwig, Far- and mid-infrared spectroscopic analysis of the substrate-induced structural dynamics of respiratory complex I, ChemPhysChem 12 (2011) 217–224.